High-Speed Germanium-Based Waveguide Electro-Absorption Modulator

P. De Heyn[1], S. A. Srinivasan[2], P. Verheyen[1], R. Loo[1], I. De Wolf[1,3], S. Balakrishnan[1], G. Lepage[1], D. Van Thourhout[2], M. Pantouvaki[1], P. Absil[1], and J. Van Campenhout[1]
[1]Imec, Kapeldreef 75, Leuven B-3001, Belgium
[2]Photonics Research Group, Dept. of Information Technology, Ghent University - Imec, St. Pietersnieuwstr. 41, 9000 Ghent, BE
[3]also at Dept. Materials Science (MTM), Faculty Engineering, KU Leuven, Belgium

Peter.DeHeyn@imec.be

Abstract: *Germanium-based waveguide electro-absorption modulators are reported in C- and L-band wavelength operation at 56Gb/s (NRZ-OOK) with extinction ratio of >3dB at 2V peak-to-peak and insertion loss below 5dB. The device is implemented in a fully integrated Si photonics platform on 200mm silicon-on-insulator wafer with 220nm top Si thickness. Wafer-scale performance data confirms the manufacturability of the device. This demonstrates the great potential for realizing high-density and low-power silicon photonic transceivers for short range interconnect.*
Keywords: *Electro-absorption modulators, optoelectronics, optical interconnects, waveguide modulators*

I. Introduction

Silicon Photonics is considered to be a key potential technology to enable the scaling of bandwidth and power density beyond the bottleneck of electrical interconnects [1]. As an important building block of the Silicon Photonics circuitry, modulators are required to have low power consumption, high modulation speed, small footprint, large optical bandwidth and robust thermal sensitivity [2]. In this paper, we review the waveguide-integrated Ge & GeSi electro-absorption modulator (EAM) operating in respectively L- and C-band showing wide open eye diagrams at 56Gb/s nonreturn-to-zero on-off keying (NRZ-OOK)[3,4]. The optimum operation point for Ge EAM devices is around 1610nm however using Ge with ~0.8% Si incorporation, the bandgap is sufficiently shifted for operation at 1550nm wavelength. The EAM devices are integrated in imec's iSiPP25G silicon photonics platform on 200mm silicon-on-insulator (SOI) wafers with 220nm top Si thickness. The Ge-based EAMs have higher optical bandwidth than Si based ring modulators and lower footprint and power consumption than the Mach–Zehnder based modulators [5].

II. Design and Fabrication

The working principle of bulk EAMs is the Franz-Keldysh (FK) effect according to which the absorption coefficient near the band edge is increased due to band-tilting caused by an applied electrical field. To enable the C-band modulation around 1550nm wavelength at room temperature, ~0.8% of Si is incorporated into Ge to shift the bandgap from 0.785eV (1580nm) to 0.808eV (1535nm). The GeSi material was selectively grown in a recessed Si region with a gas mixture of GeH_4, diluted SiH_4 and H_2 using reduced pressure chemical vapor deposition (ASM EPSILON2000). High temperature anneal was applied to the wafer to reduce the threading dislocation density and afterwards, the over-grown GeSi was planarized by chemical mechanical polishing. The modulators were fabricated in imec's silicon photonics platform with other passive and active components.
The EAM is designed with poly-Si tapers to adiabatically butt couple the light to the active Ge or GeSi region with a width of 0.6μm and a length of 40μm, as depicted in Fig.1(a). A lateral p-i-n diode design is used to generate a high electrical field on GeSi waveguide, as shown in Fig. 1(b). Fig.1(c) shows the simulated electrical field distribution at -2V and the strength in the device center is up to 60kV/cm. The thickness of the epitaxial Ge is 400nm which is slightly reduced to 300nm for the epitaxial GeSi thickness to increase the electric field even further, as well as to lower the excess loss. In both cases, the light is clearly confined in the Ge/GeSi region with the fundamental mode shown in Fig.1(d). The absorption coefficient changes with the applied electrical field, clearly illustrating the FK effect near the band edge in 400nm thick Ge (Fig.1(e)) and 300nm thick GeSi (Fig.1(f)) EAM devices. The absorption spectra for different bias voltages cross around 1580nm and 1535nm, corresponding to the HH-Γ direct band gap for respectively epitaxial Ge and GeSi on Si. In both cases, a high quality of epitaxial grown material is obtained with dark current below 100nA at -2V. In Fig.1(g), a microscopic picture of the actual fabricated device is shown.

Copyright@IEICE

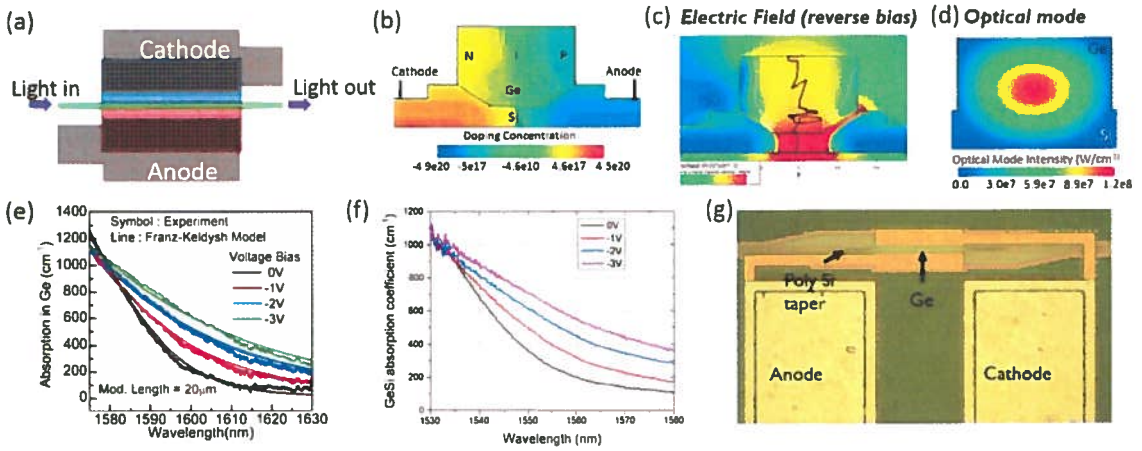

Figure 1: (a) schematic top overview (b) cross section p-i-n doping concentration (c) electric field at reverse bias (d) the main excited optical mode (e,f) measured and modelled FK effect in L- and C-band (g) microscopic picture of the fabricated device

III. STATIC MODULATOR PERFORMANCE

Fig. 2(a) shows the measured insertion loss (IL) and extinction ratio (ER) at different voltage swings measured on the GeSi EAM device in function of wavelength. The ER peaks around 1550nm. For a 2Vpp, the insertion loss is 4.8dB and the extinction ratio is 4.2dB at 1560nm. The extracted insertion loss includes the coupling loss between the Si waveguide and the GeSi modulator, the indirect band gap absorption, and FK absorption near the direct band gap due to the existing electrical field at 0V. The average ER is 4.2dB with a standard deviation of 0.3dB in 18 measured devices across a 200mm SOI wafer and the average IL is 4.4dB with a standard deviation of 0.6dB at 1560nm. Fig. 2(b) shows the extracted figure of merit (FOM) spectra at different voltage swings. The definition of FOM is ER divided by IL. The FOM peaks around 1560~1570nm. For a 2V swing, the FOM is 1.14 at 1560nm and therefore, the optimum operation wavelength for the EAM device is 1560nm. Another important device parameter is the Link Power Penalty (LPP) to quantify the operation bandwidth, defined in Ref. [4]. Fig. 2(c) shows the LPP spectra at different voltage swings. The minimum LPP value is 8.5dB and the 1dB optical bandwidth of 30nm at a 2Vpp.
The performance of the Ge EAM is very similar to the GeSi EAM with a 1dB LPP bandwidth at 2Vpp of >22nm and static ER and IL of respectively 4.6dB and 4.9dB.

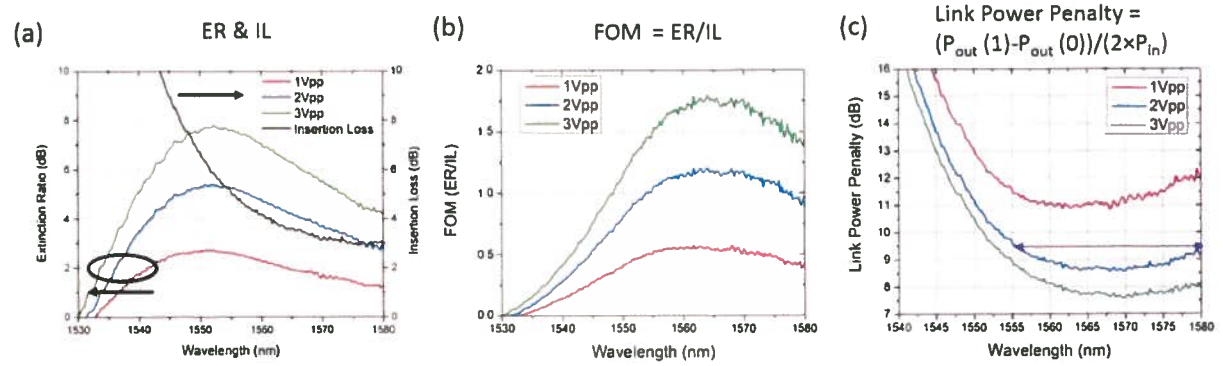

Figure 2: C-band GeSi static modulator performance in function of wavelength the GeSi EAM with in (a) the extinction ratio and insertion loss (b) the figure of merit and (c) the link power penalty. The Ge EAM has very similar performance in L-band [3].

IV. DYNAMIC MODULATOR PERFORMANCE

The 3dB bandwidth of the modulator was extracted from the electro-optic S21 measurement using a 50GHz lightwave component analyzer (LCA) with an input optical power of 3dBm. The bandwidth is greater than 50GHz for reverse bias above 1V as shown in Fig. 3(a). Since the FK effect is a sub-picosecond effect [5], the speed of the modulator is determined by the RC constant of the device. The junction capacitances is estimated to 13.8fF and 7.95fF at -1V and -2V, along with series resistances of 220Ω and 320Ω respectively. They are extracted with the help of the equivalent circuit model. These values suggest a RC limited bandwidth beyond 50GHz and further investigation is needed to explore the bandwidth limitation of these ultra-fast modulators.

Copyright@IEICE

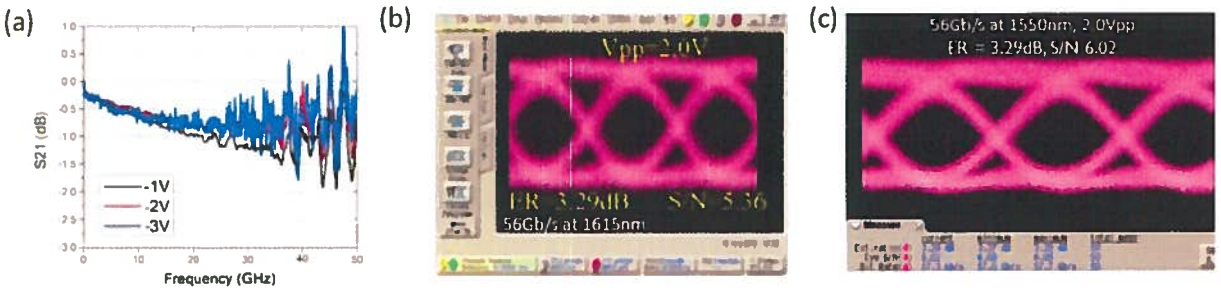

Figure 3: Dynamic modulator performance with (a) the EO - S21 measurements with varying bias at 1550nm for GeSi EAM and (b,c) 56Gb/s operation at 2Vpp and bias -1V for respectively the Ge and GeSi EAM

TABLE I: COMPARISON OF THIS WORK (*) WITH OTHER COMPETING DEVICE TECHNOLOGIES

Modulator type	Ref.	Footprint [μm^2]	Wavelength [nm]	Voltage swing [V]	Optical range [nm]	Static ER [dB]	IL [dB]	Power consumption static [mW] dynamic [fJ/bit]	3dB bandwidth GHz	Max. bit rate Gb/s
* GeSi FK	[4]	~40x10	1550	2.0	30	4.2	4.4	1.7 & 13.8	>50	50
GeSi FK	[5]	~50x10	1540	3.0	>40	5.9	4.8	11.3 & 147	38	28
* Ge Fk	[3]	~40x10	1615	2.0	>22.5	4.6	4.9	1.2 & 12.8	>50	56
Si MZM	[7]	~3000x500	1300	1.5	>80	3.4	7.1	20 & 450	30	50
Si ring	[8]	~10x10	1550	0.5	<0.1	6.4	1.2	<0.01 & 1	21	44
Si ring	[9]	~5x5	1566	2.5	<0.1	4.5	2.4	~ & 45	40	56
III-V on Si	[10]	>100x350	1300	2.2	>30	>10	4.8	6.2 & 484	74	50

V. CONCLUSIONS

We have demonstrated a 56Gb/s Ge and GeSi waveguide electro absorption modulator integrated in a 220nm SOI photonics platform for operation in respectively L- and C-band. The modulator has a 3-dB bandwidth modulation greater than 50GHz and a junction capacitance of 13.8fF at -1V. For a 2V swing, the static extinction ratio is 4.2±0.3dB, insertion loss is 4.4±0.6dB and link power penalty is 8.5dB. While operating at 56Gb/s data rate, we measure a >3.0dB dynamic extinction ratio at 2Vpp at 1610nm and 1550nm.

ACKNOWLEDGMENT

This work has been carried out as part of imec's industry-affiliation program on Optical I/O. The authors acknowledge imec's 200mm p-line for contributions to the device fabrication and imec's PDK team for mask preparation and tape-out. Device design was performed in Sentaurus TCAD, provided by Synopsys. Device layout was performed in IPKISS, provided by Luceda Photonics. The authors would like to thank Antoine Pacco and Veerle Simons for the help with GeSi material development.

REFERENCES

[1] D.A.B. Miller, "Device Requirements for Optical Interconnects to Silicon Chips", *Proc. IEEE*, vol. 97, no. 7, pp. 1166–1185, Jul. 2009.
[2] G.T. Reed, et al. "Silicon Optical Modulators", *Nat. Photon*, 4, 518 - 526 (2010).
[3] A. Srinivasan, et al. "56Gb/s Germanium Waveguide Electro-Absorption Modulator", *Lightwave Technology, Journal of*, vol.PP, no.99, pp.1-1.
[4] A. Srinivasan. et. al. "50Gb/s Germanium Waveguide Electro-Absorption Modulator", Tu3D.7, OFC 2016
[5] D. Feng, et. al. "High-speed GeSi electroabsorption modulator on the SOI waveguide platform," IEEE J. Sel. Topics Quantum Electron., vol. 19, no. 6, pp. 64–73, Nov./Dec. 2013.
[6] J.F. Lampin, et al. "Detection of picosecond electrical pulses using the intrinsic Franz–Keldysh effect", *APL* 78, 4103–4105 (2001).
[7] M. Streshinsky, et al. "Low power 50 Gb/s silicon traveling wave Mach-Zehnder modulator near 1300 nm", *Opt. Express* 21, 30350-30357, 2013.
[8] E. Timurdogan, et al. "An ultralow power athermal silicon modulator", *Nature Communications*, 5, 4008, 2014.
[9] M. Pantouvaki, et al. "56Gb/s Ring Modulator on a 300mm Silicon Photonics Platform", TH2.4.4, *ECOC* 2015
[10] Y. Tang, et al. "Over 67 GHz bandwidth hybrid silicon electroabsorption modulator with asymmetric segmented electrode for 1.3 μm transmission", *Opt. Express* 20, 11529-11535 (2012).

Copyright@IEICE

Wednesday, July 6

Room D

WD1 9:00-10:30
Active Devices on Si

Presider: Noriyuki Yokouchi (Furukawa Electric Co., Ltd., Japan)

9:00-9:30 WD1-1 (Invited)
High-Speed Germanium-Based Waveguide Electro-Absorption Modulator
P. De Heyn[1], S. A. Srinivasan[2], P. Verheyen[1], R. Loo[1], I. De Wolf[1,3], S. Balakrishnan[1], G. Lepage[1], D. Van Thourhout[2], M. Pantouvaki[1], P. Absil[1], J. Van Campenhout[1]
[1]Imec, Belgium, [2]Ghent Univ. - Imec, Belgium, [3]KU Leuven, Belgium

Germanium-based waveguide electro-absorption modulators are reported in C- and L-band wavelength operation at 56Gb/s (NRZ-OOK) with extinction ratio of >3dB at 2V peak-to-peak and insertion loss below 5dB. The device is implemented in a fully integrated Si photonics platform on 200mm silicon-on-insulator wafer with 220nm top Si thickness. Wafer-scale performance data confirms the manufacturability of the device. This demonstrates the great potential for realizing high-density and low-power silicon photonic transceivers for short range interconnect.

9:30-9:45 WD1-2
Low-Voltage Carrier-Depletion Silicon Mach-Zehnder Modulator at High Temperatures without Thermo-Electric Cooling
Norihiro Ishikura[1], Kazuhiro Goi[1], Hiroki Ishihara[1], Shinichi Sakamoto[1], Kensuke Ogawa[1], Tsung-Yang Liow[2], Xiaoguang Tu[2], Guo-Qiang Lo[2], Dim-Lee Kwong[2]
[1]Fujikura Ltd., Japan, [2]Institute of Microelectronics, Singapore

High-extinction-ratio 10-Gb/s modulation in carrier-depletion silicon Mach-Zehnder modulator is demonstrated with RF amplitude as low as 3.6 Vpp at temperatures up to 130 °C without thermo-electric cooling. Algebraic representation of DC optical characteristics is presented.

9:45-10:00 WD1-3
High-efficiency Silicon Optical Modulator Using a SiN-strip Loaded Waveguide on the Photonic SOI Platform
Guangwei Cong, Yuriko Maegami, Morifumi Ohno, Makoto Okano, Koji Yamada
National Inst. of Adv. Industrial Sci. and Tech. (AIST), Japan

We proposed a novel silicon optical modulator using the SiN-strip loaded waveguide instead of the shallow-etched rib waveguide. This modulator can show a ~2-times maximum efficiency enhancement than the conventional rib-waveguide based lateral PN modulator.

10:00-10:15 WD1-4
1.3-μm DFB Laser μ-Platform; Light Source Suitable for Silicon Photonics Platform
Takanori Suzuki[1], K. R. Tamura[2], Koichiro Adachi[1], Aki Takei[1], Akira Nakanishi[2], Kazuhiko Naoe[2], Kouji Nakahara[2], Shigehisa Tanaka[2]
[1]Hitachi, Ltd., Japan, [2]Oclaro Japan, Inc., Japan

We fabricated a light source based on a lens-integrated surface-emitting laser μ-platform for silicon photonics platforms. A low coupling loss to silicon photonics platform of 3.9dB was achieved by optimizing design of the laser μ-platform.

10:15-10:30 WD1-5
Hybrid Silicon-based Tunable Laser with Integrated Reflectivity-tunable Mirror
G. de Valicourt[1], C. Gui[1,3], A. Melikyan[1], P. Dong[1], C-M. Chang[1], A. Maho[2], R. Brenot[2], Y. K. Chen[1]
[1]Alcatel-Lucent, USA, [2]'Thales Research and Technology' and 'CEA Leti', France, [3]Huazhong Univ. of Science and Technology, China

We propose a novel hybrid silicon-based laser with integrated variable reflectivity mirror. The single-ring laser is tunable over 10 nm with high SMSR. The adjustment of the mirror reflectivity allows controlling lasers characteristics.

Room E

WE1 9:00-10:30
Nonlinear Devices

Presider: Masaya Notomi (NTT, Japan)

9:00-9:30 WE1-1 (Invited)
Advances in Second Order Nonlinear Effect in Silicon
P. Damas, X. Le Roux, M Berciano, G. Marcaud, C. Alonso-Ramos, D. Benedikovic, E. Cassan, D. Marris-Morini, L. Vivien
Univ. of Paris-Saclay, France

In this work, we present a theoretical model to determine the second order nonlinear coefficient under strain gradient in silicon. Furthermore, carrier effect due to applied electric field has also been taking into account to analyze the obtained experimental phase variation.

9:30-9:45 WE1-2
Multiple Optical Carrier Generation Using Multiple QPM Device
Kazuki Nakamura[1], Hin Channa[1], Masaki Asobe[1], Takeshi Umeki[2], Hirokazu Takenouchi[2]
[1]Tokai Univ., Japan, [2]NTT Device Technology Laboratories, Japan

Phase matching of multiple QPM $LiNbO_3$ waveguide was evaluated in the presence of high power second harmonic light. Based on the characterization, we demonstrate multiple carrier generation using multi-stage frequency mixing in multiple QPM device.

9:45-10:00 WE1-3
Fabrication of High Optical Quality Factor Free-Standing As_2S_3 Microdisk Resonators on a Silicon Chip
Mingxiao Zhao[1], Mingming Zhao[1], Xiaoshun Jiang[1], Yuan Chen[1], Jiyang Ma[1], Min Xiao[1,2]
[1]Nanjing Univ., China., [2]Univ. of Arkansas, USA

We demonstrate a chip-based free-standing As_2S_3 microdisk resonator with a Q-factor of 9.8×10^5. The critical coupling condition is achieved by efficiently coupling the modes of the microresonator with a tapered optical fiber.

10:00-10:15 WE1-4
Wavelength Modulation Spectroscopy of Formaldehyde Using 3μm DFG Laser
Ryohei Fujisawa[1], Masaki Asobe[1], Akira Katoh[1], Shigeru Yamaguchi[1], Akio Tokura[2], Hirokazu Takenouchi[2]
[1]Tokai Univ., Japan, [2]NTT Corporation, Japan

Effect of modulation condition of 3μm DFG laser on intensity noise in wavelength modulation spectroscopy was studied. The reduction of the intensity noise enabled real time detection of formaldehyde without baseline subtraction.

10:15-10:30 WE1-5
Chirp-free Spectral Compression of Parabolic Pulses in Silicon Nitride Channel Waveguides
Chao Mei, Jinhui Yuan, Kuiru Wang, Xinzhu Sang, Chongxiu Yu
[1]Beijng Univ. of Posts and Teleommunications, China, [2]Hong Kong Polytechnic Univ., Hong Kong

A practical scheme is presented to achieve spectral compression of highly chirped parabolic pulses in a 4-cm long Si_3N_4 channel waveguides. Chirp-free pulses with -15.5-dB pedestals and a compression ratio of 25.4 are obtained.

Room F

WF1 9:00-10:30
Photonic Switching Technology (I)

Presider: Katsuyuki Utaka (Waseda Univ., Japan)

9:00-9:30 WF1-1 (Invited)
NxN Wavelength Selective Switches
Hisato Uetsuka[1], Shu Namiki[1], Keiichi Sasaki[2]
[1]National Institute of Advanced Industrial Science and Technology (AIST), Japan, [2]Kitanihon Electric Cable Corporation, LTD, Japan

A 5x5 Wavelength Selective Switch (WSS) is proposed and demonstrated. The cross-connect optics has the orthogonal imaging systems operating in the switching plane and the dispersion one differently. The switching plane has the 2f-Fourier optics with Rayleigh length. On the other hand, the dispersion plane has the 4f- imaging optics. Two types of switching engine, as MEMS Mirrors and Liquid Crystal on Silicon (LCOS) are applied for the same cross-connect optics. The WSS with MEMS Mirrors has the 100GHz channel spacing compatible to the ITU-grid. On the other hand, the WSS with LCOS has the variable channel spacing.

9:30-9:45 WF1-2
Wavelength Selective Switch for Multi-core Fiber Based Space Division Multiplexed Network with Core-by-core Switching Capability
Kenya Suzuki, Mitsumasa Nakajima, Keita Yamaguchi, Goh Takashi, Yuichiro Ikuma, Kota Shikama, Yuzo Ishii, Mikitaka Itoh, Mitsunori Fukutoku, Toshikazu Hashimoto, Yutaka Miyamoto
NTT Corporation, Japan

We demonstrate a 7-core-MCF 1x4 wavelength selective switch (WSS) for a space division multiplexed network with core-by-core switching capability by a WSS multiplexing technique using spatial and planar optical circuit platform with a laser-inscribed fan-in/fan-out.

9:45-10:00 WF1-3
Demonstration of 1,440x1,440 Fast Optical Circuit Switch for Datacenter Networking
Koh Ueda[1], Yojiro Mori[1], Hiroshi Hasegawa[1], Hiroyuki Matsuura[2], Kiyo Ishii[2], Haruhiko Kuwatsuka[2], Shu Namiki[2], Toshio Watanabe[3], Ken-ichi Sato[2,1]
[1]Nagoya Univ., Japan, [2]National Institute of Advanced Industrial Science and Technology (AIST), Japan, [3]NTT Device Innovation Center, Japan

We propose a fast and large-scale optical circuit-switch architecture for intra-datacenter applications. A 1,440x1,440 optical switch is designed and tested with 180-wavelength signals in the full C band; the worst switching time is 498 microseconds.

10:00-10:15 WF1-4
32x32 Silicon Photonic Switch
Dritan Celo[1], Dominic J. Goodwill[1], Jia Jiang[1], Patrick Dumais[1], Chunshu Zhang[1], Fei Zhao[2], Xin Tu[2], Chunhui Zhang[2], Shengyong Yan[2], Jifang He[2], Ming Li[2], Wanyuan Liu[2], Yuming Wei[2], Dongyu Geng[2], Hamid Mehrvar[1], Eric Bernier[2]
[1]Huawei Technologies Canada Co., Ltd., Canada, [2]Huawei Technologies Co. Ltd., China

Lightpaths are switched in a 32×32 silicon photonic switch, with 448 thermo-optic Mach-Zehnders and 864 monolithic monitor photodiodes. It is packaged in a CBGA with 68-fiber ribbon, and every cell has an off-chip control circuit.

10:15-10:30 WF1-5
Silicon Photonics Optical Switch based on Ring Resonator
Antoine Descos[1], M. Ashkan Seyedi[1], Chin-Hui Chen[1], Marco Fiorentino[1], François Vincent[2], David Penkler[2,3], Bertrand Szelag[3], Raymond G. Beausoleil[1]
[1]Hewlett Packard Labs, USA, [2]Hewlett Packard Enterprise, France, [3]CEA-LETI, France

Optical switches based on ring resonator cavities are fabricated in a silicon photonics foundry process and analyzed. Effective switching with P-i-N junction is shown for a 20Gbps signal with a bias voltage as low as 1 volt.